Disturbed Matrix Metalloproteinase Activity of Bruch's Membrane in Age-Related Macular Degeneration

Ali A. Hussain, Yunhee Lee, Jin-Jun Zhang, and John Marshall

Purpose. To evaluate the potential role of the matrix metalloproteinase (MMP) system of Bruch's membrane in the pathology of age-related macular degeneration.

Methods. Free and bound pools of gelatinase activity in Bruch's membrane–choroid preparations were isolated by phosphate-buffered saline (PBS) and sodium dodecyl sulfate (SDS) extraction, respectively. Individual MMP species were separated by gelatin-substrate zymography and the levels were quantified by densitometric techniques. Altogether, 13 control (age range, 71–99 years) and 6 AMD (age range, 71–95 years) donor eyes were used.

Results. All the gelatinase components normally present in control samples were also present in AMD tissue without any significant differences in their molecular masses. Total levels (bound plus free) of active MMP2 and -9 were significantly reduced in AMD donors ($P < 0.05$). The decrease in active MMP2 may be attributable to a similar reduction in the level of free pro-MMP2, the precursor to the active form. Reduction in active MMP9 occurred despite a nearly 3.5-fold increase in free pro-MMP9. The high-molecular-mass gelatinases denoted by HMW1 and -2 and comprising homo- and heteropolymers of pro-MMP2 and -9 were also raised in AMD ($P < 0.05$). The sequestration of free pro-MMP2 and -9 by these high-molecular-mass complexes may further contribute to reduced rates of activation of MMPs.

Conclusions. The reduction in the levels of activated MMP2 and -9 may be responsible for impaired matrix degradation of Bruch's membrane, leading to the pathology associated with AMD. The degradation pathway is therefore a viable therapeutic target for future intervention. (*Invest Ophthalmol Vis Sci.* 2011;52:4459–4466) DOI:10.1167/iovs.10-6678

The structural and functional characteristics of most extracellular matrices (ECMs) are maintained by tightly coupled processes of synthesis and degradation.[1,2] The degradation pathway is mediated by a family of 24 Zn^{2+}-containing, Ca^{2+}-dependent proteolytic enzymes referred to as the matrix metalloproteinases (MMPs). These MMPs are released as inactive proenzymes and on activation (by proteolytic cleavage of a small peptide) are capable of digesting all components of an ECM.[3–6] The catalytic activity of MMPs is checked by a family of small peptides called the tissue inhibitors of MMPs (TIMPs).

From the Division of Molecular Therapy, UCL Institute of Ophthalmology, University of London, London, United Kingdom.

Supported by Fight for Sight UK and Guide Dogs for the Blind UK.

Submitted for publication October 4, 2010; revised January 24, 2011; accepted March 12, 2011.

Disclosure: **A.A. Hussain**, None; **Y. Lee**, None; **J.-J. Zhang**, None; **J. Marshall**, None

Corresponding author: Ali A. Hussain, Division of Molecular Therapy, UCL Institute of Ophthalmology, 11-43 Bath Street, London EC1V 9EL; alyhussain@aol.com.

The secretion of MMP1, -2, -3, and -9 by retinal pigment epithelial (RPE) and choroidal endothelial cells and their presence in Bruch's membrane has been demonstrated.[7–10] Also TIMP1 and -2 have been shown to be freely mobile within Bruch's, with TIMP3 being tightly bound to the matrix.[9,11] Thus, Bruch's membrane has been shown to contain all the components of the degradation machinery required for continuous turnover of the ECM to maintain its functional characteristics.

Abnormalities in either the biosynthetic or degradation pathways for ECM turnover or in constituents interacting with the degradation pathway have the potential to alter the morphologic and functional characteristics of Bruch's membrane. Thus, in Sorsby's fundus dystrophy, a mutation in the TIMP3 gene leads to an early-onset form of macular degeneration characterized by a thick (~30 μm) deposition of lipid-rich material on top of the membrane.[12,13] Although the mechanism of degeneration is not known, it is likely that the extensive accumulation of the abnormal TIMP3 molecule inhibits the degradative capacity, leading to the deposition of the lipid-rich layer which in turn compromises diffusional support of the photoreceptor cells. Similarly, mutations in molecules that normally interact with the MMP system can also lead to abnormal ECM turnover.[14] Thus, a mutation in the TIMP-3 binding epidermal fibulin-like extracellular matrix protein 1 (EFEMP1) is responsible for the hereditary macular degenerative disease Malattia Leventinese.[15]

In normal ageing, the increased thickness of Bruch's membrane,[16,17] the deposition of normal and abnormal ECM material,[18] the increased cross-link formation (oxidative and nonenzymic glycosylation leading to advanced glycation end products [AGEs] and advanced lipoxidation end products [ALEs]),[19] and the accumulation of lipid-rich debris[20,21] are changes that imply a disturbance in the ECM turnover of the membrane. A contributory factor for reduced degradation may be the age-related increase in the level of TIMP3.[22] This increase is somewhat counterbalanced by an increase in the levels of pro-MMP2 and -9.[10]

Although levels of pro-MMP2 and -9 have been shown to increase with age,[10] this change does not imply greater degradation potential, since it is the activated forms of the enzymes that are catalytically effective. Other players capable of modifying the degradation process are the AGEs and ALEs, since they are known to be potent inhibitors of MMP activity.[23–25] Furthermore, the age-related increase in intermolecular fibril cross-links has been shown to reduce the susceptibility of the collagen molecule to proteolytic action.[26,27]

These normal ageing changes affect the functional characteristics of Bruch's membrane, leading to a reduction in the transport of fluids, amino acids, and larger molecular complexes (essential carrier bound metals, vitamins, and lipids).[28–32] This reduction in transport also implies impaired removal of membranous debris extruded by the RPE, and thus a vicious cycle is set up that has the potential to undermine the normal homeostatic support of the overlying photoreceptor

layer. Clinically, reduced transport status is often indicated by reduced scotopic thresholds in the elderly and in those with early maculopathy due to reduced efficiency in the transport of vitamin A.[33–36]

In advanced ageing, associated with age-related macular degeneration (AMD), structural and functional alterations are more exaggerated, leading to a further decrease in transport functions.[32] Diminished metabolic support may therefore be the initial insult that progresses to the death of RPE and photoreceptors, incurring additional inflammatory or neovascular episodes. In AMD, TIMP3 levels were considerably elevated compared with age-matched controls with the consensus being that elevated TIMP3/MMP ratios may underlie the increased thickening of Bruch's membrane in this condition.[11,22] Involvement of the MMP system in the etiology of AMD has also been inferred from the raised levels of plasma pro-MMP9 in these patients.[37]

Furthermore, polymorphisms in the promoter region of the MMP9 gene appear to dictate the transcriptional activity of this enzyme.[38–40] Thus, in mesangial cells of mice, 24 repeats of the cytosine-adenine (CA) sequence in the promoter region have been associated with a 20 times higher expression of pro-MMP9, compared with that in strains with 20 CA repeats.[41] An association between the length of the MMP9 promoter microsatellites and choroidal neovascularization has been documented, and alleles with 22 or more CA repeats were more often found in AMD patients.[42]

The gelatinase system of Bruch's membrane appears to be far more complex than previously envisioned. Thus, in addition to the monomeric species of pro- and active-MMP2 and -9, high-molecular-mass species (termed HMW1 and -2), thought to be homo- and/or heteropolymers of monomeric pro-MMPs have also been identified.[43,44] A much larger, macromolecular MMP complex (LMMC), comprising primarily HMW1, HMW2, and pro-MMP9, together with some pro-MMP2, has also been shown to be present in human Bruch's membrane.[44] Further complications relate to the compartmentalization of these species between bound and free pools. These observations introduce the concept of sequestration of MMPs, thereby effectively removing them from the activation process. Our current understanding of the interrelationships between the various gelatinases species of Bruch's membrane is given in Figure 1.

The present investigation was therefore designed to screen donor tissue and clarify any disturbance (if present) in the gelatinase component of the MMP degradation system of Bruch's membrane from donors with AMD. Peripheral samples of Bruch's-choroid were obtained from 6 AMD (age range, 71–95 years) and 13 control (age range, 71–99 years) donor eyes, and the level of gelatinase species in the free and bound fractions was quantified by zymographic methods.

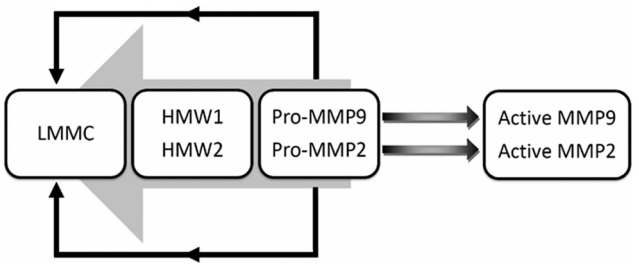

FIGURE 1. The gelatinase pathway in human RPE-Bruch's-choroid. The gelatinase components comprise the pro- and active- forms of the monomeric MMP2 and -9, the polymeric forms denoted by HMW1 and -2 and the macromolecular MMP complex termed LMMC consisting of HMW1 and -2, and pro-MMP2 and -9. Apart from LMMC, all other gelatinase components have been shown to exist in bound and free states. Pathway constructed from Hussain et al.[44]

METHODS

Tissue Preparation

Human donor eyes, with consent granted for research, (13 pairs, age range, 71–99 years and postmortem times 24–48 hours) were obtained from the Bristol Eye Bank (United Kingdom). In addition, six AMD donor eyes (ages 71, 79, 81, 83, 87, and 95 years) were obtained through the Macular Disease Society Eye Donor Scheme (United Kingdom). Clinical data sheets accompanied the AMD donor eyes, and their status was confirmed by fundus examination during the dissection procedure. The corneas were removed for use in transplantation surgery and the remaining globes were transported to the laboratory on saline-moistened pads in an ice chest. The donor eyes were managed in compliance with the Declaration of Helsinki for research involving human tissue.

After a preliminary fundus examination with a dissecting microscope, to ensure that the control eyes were free from disease and gross handling artifacts, a circumferential incision was made 5 mm posterior to the scleral sulcus, and the remaining anterior segment, lens, and vitreous were discarded. The macular region was located, and the posterior globe was opened in the shape of a Maltese cross, such that one of the quadrants housed the optic disc and the foveal pit. An 8-mm, full-thickness, trephined disc was removed from the periphery of this quadrant and transferred to a Petri dish containing phosphate-buffered saline (PBS; Sigma-Aldrich, Poole, UK). The neural retina was easily detached and discarded exposing the monolayer of RPE cells. These were gently brushed away with the aid of a camel's hair brush. Finally, under low-power magnification, the Bruch's–choroid complex was carefully removed from the underlying sclera by blunt dissection. After a quick rinse in fresh PBS, the tissue sample was placed in a 1.5-mL tube (Eppendorf, Hamburg, Germany) and stored at −70°C. The same procedure was used to obtain 8-mm discs of peripheral Bruch's-choroid from AMD donor eyes.

Sample Preparation for Zymography

For extraction of free and bound pools of gelatinase species, 100 μL of PBS was added to each sample, and the tubes were vortexed five times for periods of 1 minute each. The samples were then centrifuged for 5 minutes at 10,000*g* ,and the supernatant, representing the free pool of MMPs, was removed. Twenty microliters of the supernatant was mixed with 40 μL of nonreducing SDS sample buffer (Invitrogen, UK), and 20 μL of this mixture was applied to zymographic gels.

The pellet from the centrifugation was washed several times with 1.0-mL aliquots of PBS and reconstituted with 20 μL water and 40 μL nonreducing SDS sample buffer. The samples were vortexed as before and spun at 10,000*g* for 5 minutes, and 20 μL of the supernatant representing the bound or SDS-extracted fraction was applied to zymography gels.

Zymography

For zymography, 10% SDS-PAGE gels (1.0 mm thick) were prepared containing a 4% stacking layer and 0.1% gelatin in the separating layer. Samples for analysis were loaded into lanes together with prestained protein molecular mass markers, spanning a range of 6 to 500 kDa (Invitrogen, Paisley, UK and 20% fetal calf serum (FCS; Sigma-Aldrich) as an internal standard to correct for gel-to-gel variation in staining intensity. Electrophoresis was then performed (X Cell SureLock Mini-Cell system; Invitrogen).

After electrophoresis (150 V, 1 hour), the gels were removed from their cassettes, rinsed in distilled water, and incubated for two half-hour periods in 2.5% Triton X-100, to remove SDS and renature the proteins. They were then transferred to reaction buffer (50 mM Tris-HCl, 10 mM $CaCl_2$, 75 mM NaCl, and 0.02% NaN_3, pH 7.4) and incubated at 37°C for 20 hours, to allow proteolytic digestion of the gelatin substrate. The gels were rinsed again in distilled water and stained with dye containing Coomassie blue G-250 (SimplyBlue

SafeStain; Invitrogen) for a period of 3 hours. Destaining was performed in distilled water for 1.5 hours.

Gelatinase activity was observed as clear bands on a blue background. These gels were scanned at a resolution of 2400 dpi (3490 scanner; Epson, Hemel Hempstead, UK) and stored in JPEG format. The color images were uploaded into a computer running gel analysis software (Quantiscan, ver. 3.0; Biosoft, Cambridge, UK) in gray-scale format, and the colors were inverted so that the MMPs were now visualized as dark bands against a whitish background. The software then generated a densitometric profile of each lane and calculated the area under individual gelatinase bands. This integrated area has been shown to relate directly to the amount of gelatin hydrolyzed.[10] For normalization to control for gel-to-gel variation in staining intensity, the pro-MMP9 band of the fetal calf serum sample was chosen as a reference since the alternative pro-MMP2 band often showed distortion and skewing effects. Areas under the various gelatinase bands were thus normalized and corrected for dilution, allowing the expression of MMP activity as gelatinase band area per 8-mm disc of tissue.

Statistical Analysis

Data are presented as the mean ± SD. The Mann-Whitney test was used to assess significant differences ($P < 0.05$; $P < 0.01$or $P < 0.005$) between control and AMD samples (add-in XLStat statistical analysis software for Microsoft Excel; Addinsoft, Andernach, Germany).

Results

Gelatinase activity in both free and bound compartments of Bruch's–choroid preparations was assessed by zymography, and the resulting zymograms (gray scaled and color inverted) were collated from the different gels and are presented in Figure 2. All gels were aligned with respect to the position of the molecular size markers included in each gel.

The free pool of gelatinases released (Fig. 2A) was marked by the absence of active MMP-9 from both AMD and control donors. A visual inspection of the gels showed levels of pro-MMP9 to be elevated in AMD donors, whereas levels of pro-MMP2 were reduced. The migratory distances of HMW2, HMW1, and pro- and active MMP2 were virtually the same within and between donor subsets. However, the migratory distances of pro-MMP9 showed a detectable variation within each donor set.

In the bound pool (Fig. 2A), gelatinase activities were much higher than in the free pool. Levels of HMW2, HMW1, and pro-MMP9 were greater in the AMD donor group. On the other hand, levels of pro- and active MMP2 species were generally lower in the AMD group.

The variability in the migratory distances of pro-MMP9 observed in the free pool was much clearer in the bound samples, due to the higher level of enzymatic activity. A comparison of the positions of the pro-MMP9 bands in AMD donors aged 71 and 83 years suggested the presence of two adjacent bands in the latter. The presence of two proteins running close to each other was also indicated on gels for the 87-year-old AMD donor, and control donors aged 94, 80a, and 71 years. The likelihood of two adjacent protein bands can also be inferred by comparing the 98-year-old control band with neighboring lanes for the 80a- and 99-year-old samples. In the present study, no attempt was made to separate these bands, and the midpoint was used in determining the molecular masses.

In the control bound pool, active MMP-9 was discernible as a narrow distinct band but in AMD samples, such specific banding was less frequently observed and replaced by a broader smear (Fig. 2B). Representative densitometric gel scans of control samples show clearly identifiable active MMP-9 peaks (Figs. 3a, 3b). Scans of AMD samples were generally dominated by a gradation of activated species that appeared as smears on the zymograms (Figs. 3c, 3d).

The gel scan for the bound fraction in the 95-year-old AMD donor (Fig. 3c) suggests that the pro-MMP9 band actually housed two gelatinase species, since the scan profile for this species was not symmetric around the expected position for

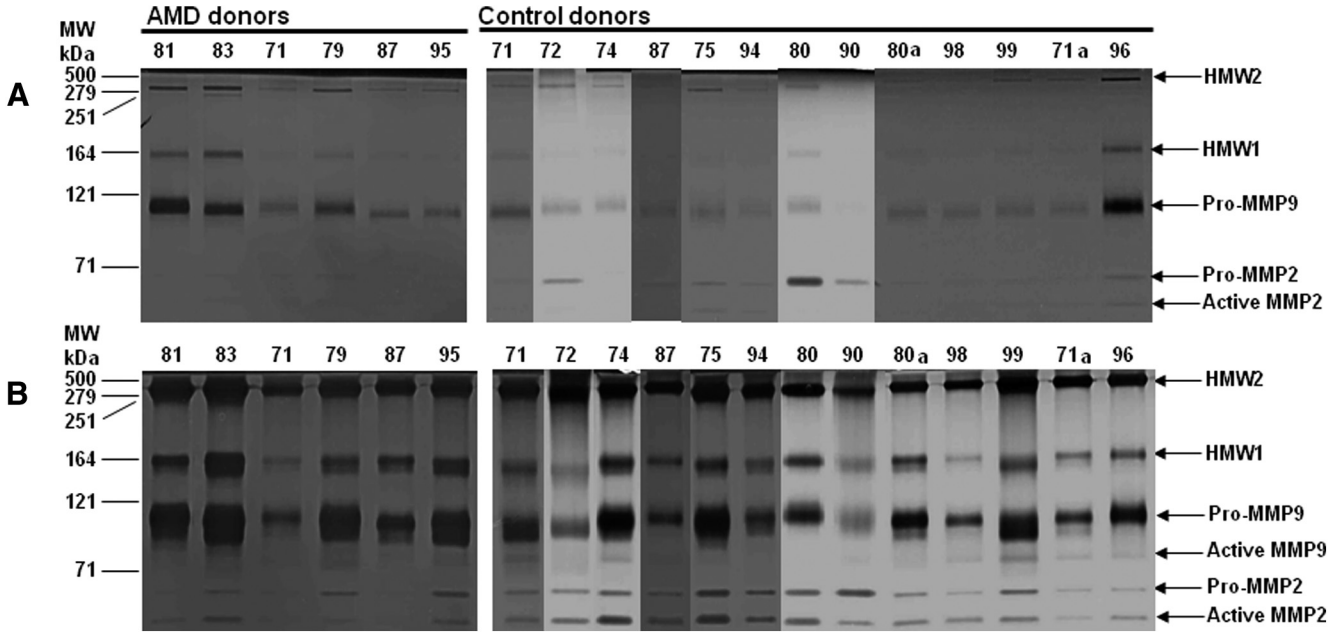

Figure 2. Zymographic analysis of the gelatinase component of Bruch's-choroid preparations. The gelatinase species from 13 control (age range, 71–99 years) and six AMD (age-range, 71–95 years) donor eyes were fractionated into the free (**A**) and bound (**B**) pools, by PBS and SDS extraction, respectively. The stained gels were gray scaled and color inverted to show gelatinase bands as dark on a whitish background. Individual gels and gel lanes have been aligned for comparison based on the positions of the molecular size markers. High-molecular-mass species were scarce, and active MMP9 was not detected in any of the samples in the free pool. The pro-MMP9 band in the bound fraction showed heterogeneity, suggesting the existence of two isoforms for the enzyme.

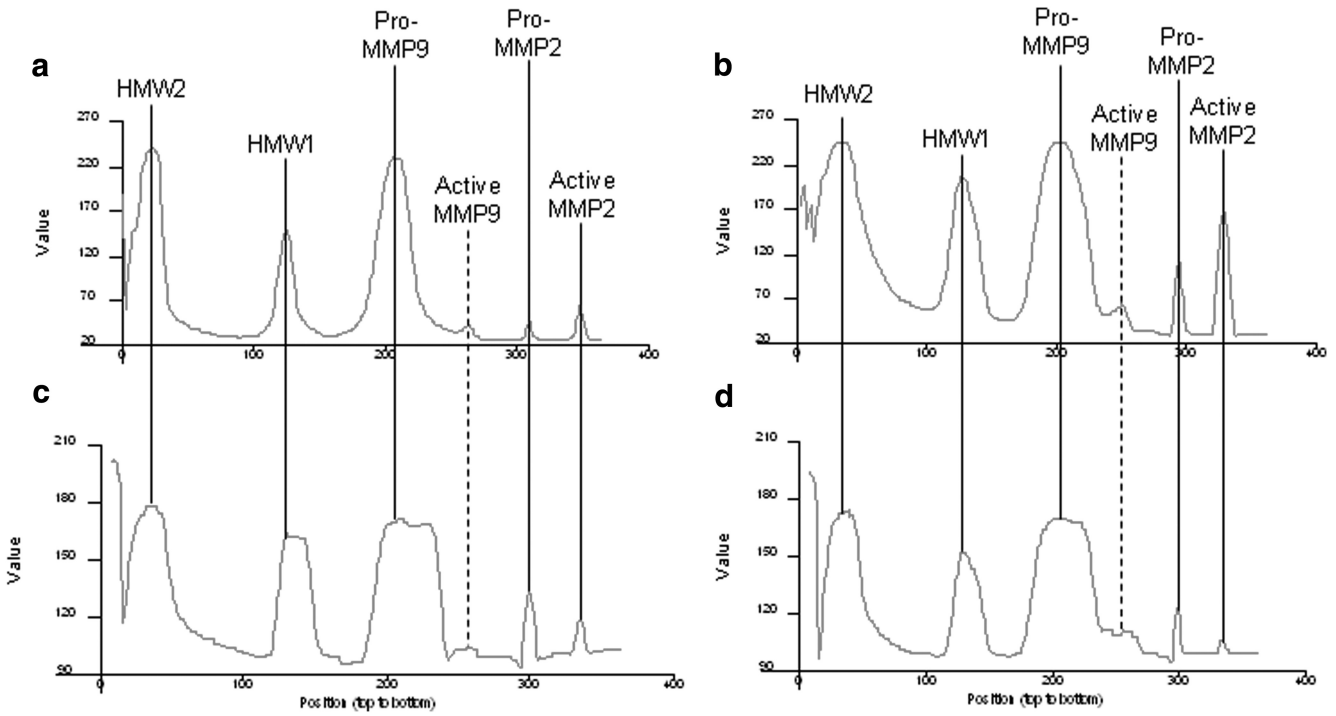

FIGURE 3. Representative densitometric scans of zymographic lanes in the bound fraction analysis of Figure 2B. Scans (**a**) and (**b**) were obtained from control donor eyes aged 96 and 74 years and scans (**c**) and (**d**) from AMD donor eyes aged 95 and 79 years, respectively. Active MMP9 species in control samples were represented by well-defined peaks whereas in the AMD eyes, they were much broader and appeared segmented. Note the expanded vertical scale in the AMD scans.

pro-MMP9 depicted in Fig. 3a. The presence of a lower molecular mass pro-MMP9 species may also be responsible for the shift in the polymeric HMW1 form (compare Fig. 3c with 3a). In other samples (Figs. 3b, 3d) the presence of a single pro-MMP9 species can be discerned since the scan profile remained symmetrically aligned around the expected position on the gel.

The molecular masses of individual gelatinase species were determined from standard logarithmic plots of relative migratory distance versus molecular mass, and there was no statistically significant difference in the gelatinase species from AMD and control donors (Table 1).

A quantitative analysis of the level of individual gelatinase species of Bruch's–choroid preparations in terms of the free, bound, and total pools is given in Table 2. There was considerable variation in levels within each donor group, and this was reflected in the large standard deviations for a given species. A better representation of the variability in the data is provided by the box-and-whisker plots in Figure 4.

The total level of the high-molecular-mass gelatinases HMW1 and -2, was significantly raised in donors with AMD ($P < 0.05$). In the absence of a statistically significant increase in bound levels, the observed increase in total levels was due primarily to an increase in free levels of HMW1 and -2 ($P < 0.01$ and $P < 0.05$, respectively).

Levels of free pro-MMP9 were significantly increased in AMD donor tissue ($P < 0.005$), doubling the total content of this MMP compared with the controls ($P < 0.05$). Despite this increase in the pro-form, active MMP9 levels were reduced ($P < 0.05$).

The free and total level of pro-MMP2 was reduced in AMD ($P < 0.05$). Also apparent in AMD samples was the reduction in bound and total levels of active MMP-2 ($P < 0.005$ and $P < 0.05$, respectively).

DISCUSSION

The zymographic analysis has demonstrated a disturbance in the gelatinase machinery of Bruch's-choroid preparations from donors with AMD. More specifically, the total levels of active MMP-2 and -9, enzymic forms responsible for proteolysis, were

TABLE 1. The Molecular Weight of Individual Gelatinase Species in the Free and Bound Pools of Bruch's Choroid Preparations

	HMW2	HMW1	Pro-MMP9	Active MMP9	Pro-MMP2	Active MMP2
Free pool						
Control	322 ± 40	162 ± 8	95 ± 2	—	65 ± 1	58 ± 1
AMD	338 ± 34	164 ± 3	97 ± 3	—	66 ± 1	59 (1)
Bound pool						
Control	323 ± 52	161 ± 7	92 ± 3	82 ± 2	65 ± 1	58 ± 1
AMD	327 ± 14	162 ± 5	94 ± 3	84 ± 2	65 ± 1	58 ± 1

Data are mean molecular masses in kilodaltons ± SD. Logarithmic plots of relative migratory distance versus molecular weight for standards were used to calculate the molecular masses of individual species. There was no significant difference between species derived from AMD and control donors.

TABLE 2. Gelatinase Activity in Peripheral Samples of Bruch's Choroid in Control and AMD Donors

MMP Species	Donor Group	Free	Bound	Total
HMW2				
	Control	1435 ± 1520	12702 ± 3940	14137 ± 4725
	AMD	6685 ± 5444*	15195 ± 3018	21880 ± 8182*
HMW1				
	Control	1335 ± 2470	5996 ± 2911	7331 ± 4040
	AMD	6327 ± 7064†	10480 ± 5616	16807 ± 11950*
Pro-MMP-9				
	Control	9354 ± 11895	16068 ± 7692	25422 ± 16553
	AMD	33375 ± 25579‡	22572 ± 7274	55947 ± 30662*
Pro-MMP-2				
	Control	1567 ± 1753	1393 ± 964	2960 ± 2071
	AMD	379 ± 374*	674 ± 700	1053 ± 854*
Active MMP-9				
	Control	NDet	517 ± 376	517 ± 376
	AMD		195 ± 80*	195 ± 80*
Active MMP-2				
	Control	357 ± 428	1978 ± 1140	2336 ± 1257
	AMD	335 ± 519	614 ± 534‡	949 ± 885*

Densitometric scans of individual MMP species were corrected for dilution procedures, background, and with respect to the fetal calf serum standard and are expressed as mean area ± SD per 8-mm-diameter disc of tissue. Statistical significance was assessed by the Mann-Whitney nonparametric test. The high-molecular-mass species (HMW1 and -2) and pro-MMP9 were significantly increased in AMD donors, primarily because of elevations in the free pool. On the other hand, levels of pro-MMP2 were significantly lower in AMD. Levels of active MMP2 and -9 were significantly reduced in AMD donors. ND, not detected.

* $P < 0.05$.

† $P < 0.01$.

‡ $P < 0.005$.

significantly reduced, diminishing the degradative capacity that is essential for maintaining the structural and functional characteristics of Bruch's membrane.

Lowered levels of active MMP2 may be a reflection of the lowered levels of the precursor, pro-MMP2. The activation mechanism for pro-MMP2 has been studied and is mediated by another metalloproteinase, a transmembrane enzyme MMP-14, in combination with TIMP2.[45–47] The activation takes place on the basolateral surface of the RPE and requires two molecules of MMP14. The first MMP14 molecule binds TIMP2 and this enables the formation of the ternary complex with pro-MMP2. A second MMP14 molecule then cleaves the pro-form to release active MMP2.[46–48] Thus, efficient activation requires the presence of MMPs and TIMPs in optimum concentrations near the basolateral surface of the RPE. The lowered levels of free pro-MMP2 ($P < 0.05$) observed for donors with AMD would therefore reduce the rate of activation leading to a reduction in total active MMP2. Lowered levels of pro-MMP2 may be the

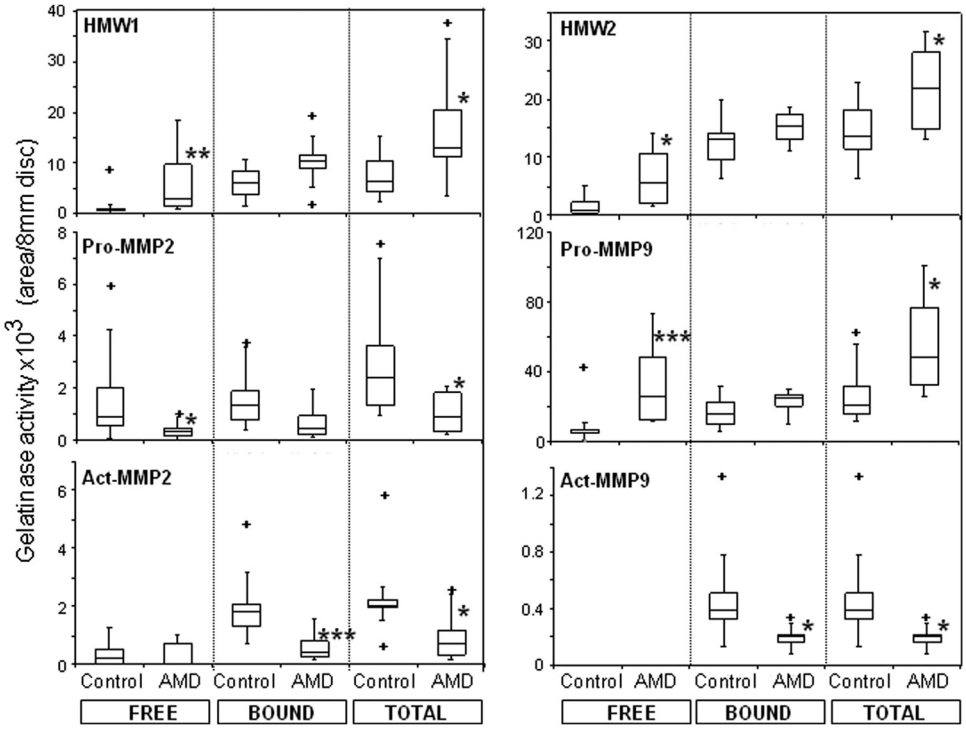

FIGURE 4. Box-and-whisker plots of individual gelatinase levels in control and AMD donor Bruch's-choroid preparations. Median, quartiles, and interquartile ranges (IQR) were determined from the data in Table 2. The ends of the whiskers were set at 1.5 × IQR above the third quartile (Q3) and 1.5 × IQR below the first quartile (Q1). The maximum and minimum values, if outside the whisker range, are shown as +. * $P < 0.05$; ** $P < 0.01$; *** $P < 0.005$.

consequence of greater sequestration culminating in raised levels of HMW1 and -2. These results support the proposal that decreased levels of active MMP2 contribute to the thickening of Bruch's membrane in the atrophic form of AMD.[10,49,50]

Regulatory mechanisms for the synthesis of pro-MMP9 and its activation are poorly understood. Current evidence suggests that the level of MMPs is dependent on transcriptional regulation, since most MMP genes are expressed in response to active physiological or pathologic tissue modeling.[4,51] In addition, basal levels of pro-MMP9 are determined by polymorphisms in the sequence of cytosine-adenine (CA) repeats in the promoter microsatellite region of the MMP9 gene.[39] Thus, in mice, mesangial cells carrying 24 CA repeats expressed MMP9 at levels nearly 20 times that of the same cells of a strain with 20 CA repeats.[41] In the human population, the number of CA repeats range from 13 to 27, with modes at 14 and 21 repeats, and a third of the population has 22 or more CA repeats.[38,52,53] Alleles with 22 or more CA repeats were shown to be more frequent in patients with AMD.[42] This association between the higher CA repeats and AMD could explain the raised levels of plasma MMP9 in these patients.[37]

The total amount (i.e., free+bound) of pro-MMP9 in Bruch's membranes of donor eyes with the AMD was elevated nearly 2.2-fold compared with that in controls ($P < 0.05$). This increase refers only to the uncomplexed pro-MMP9. The HMW1 and -2 species represent polymeric forms of pro-MMP2 and -9,[43] and since these levels were also elevated in AMD donors ($P < 0.05$), the overall increase in pro-MMP9 must be much higher.

Despite the considerably elevated levels of pro-MMP9, active MMP9 levels were significantly reduced in AMD ($P < 0.05$). The reduction in active MMP2 discussed above could be explained by the fact that levels of free pro-MMP2 were also decreased. In the case of active MMP9, however, the free levels of pro-MMP9 were actually raised nearly 3.5-fold ($P < 0.005$). This discrepancy may be related to the fact that the measured free pool of pro-MMP9 is not necessarily accurate. As shown previously,[44] HMW1 and -2 and pro-MMP-2 and -9 aggregate to form large macromolecular complexes (LMMCs), and these are released by PBS extraction into the free pool. However, on solubilization in SDS sample buffer for zymography, this complex breaks up, releasing its content of pro-MMP9 molecules. Thus, the free pool of pro-MMP9 in Table 2 is an overestimation. Further work is required to estimate the contribution of the LMMC species to the free pools of both pro-MMP9 and pro-MMP2.

Normal activation of the 92-kDa pro-MMP9 results in a partially active 88-kDa transitional intermediate, leading to the fully activated 84-kDa MMP9 molecule.[54] On the zymographic gels (Fig. 2), this 84-kDa activated species was distinctly evident in control donor eyes, but in AMD eyes was replaced by a broader smearing of the band. Densitometric scanning of electrophoretic bands due to a single protein species normally results in a Gaussian bell-shaped profile. In the active MMP9 region in AMD samples, the Gaussian profile was absent suggesting the presence of several intermediates. Whereas the transition from inactive pro-MMP9 to the fully activated 84-kDa MMP9 molecule was clearly apparent in the control samples, a more transitory presence was evident in the AMD samples, perhaps suggestive of problems with the activation process in these donors. It would be best to activate MMP samples from AMD donors with aminophenylmercuric acetate and follow the transitory conversion by zymography according to the methodology of Guo et al.[10]

The present investigation was undertaken with samples derived from the peripheral fundus. The peripheral fundus was sampled because in AMD eyes, the presence of scar formation in the macular region due to the advanced nature of the disease in these aged eyes made it virtually impossible to isolate intact specimens. In control donors, the ageing changes observed at macular locations were more advanced than at peripheral locations. Functional parameters of Bruch's membrane such as the hydraulic transport of fluids and the diffusional transport of high-molecular-mass dextrans declined at faster rates in the macular region.[28,29,32] Similarly, while active MMP2 species were frequently observed in the periphery, they were only occasionally encountered in macular locations.[10] If the macular–peripheral difference in control donors also existed in AMD, then the changes in the gelatinase components in macular regions of these patients would be expected to be much more severe.

The physiological effects of a reduction in active MMP2 and -9 in Bruch's membranes of the AMD eyes would be augmented by the increased levels of TIMP-3 inhibitor,[22] inhibition by increased levels of AGEs and ALEs,[23] and the reduced susceptibility to proteolytic action by the highly cross-linked nature of the altered collagen molecule.[27] The resulting degenerative changes in Bruch's membrane would be expected to initially affect the metabolic exchange processes of the membrane. An early disturbance appears to be in the carrier mediated transport of vitamin A, giving rise to reduced scotopic thresholds in the very elderly and to early maculopathy.[33–36] A further compromise in the homeostatic mechanisms for exchange of nutritional and waste products across Bruch's membrane is expected initially to affect the RPE, followed by deterioration in photoreceptor function.

The degenerative changes in functional parameters of Bruch's membrane associated with normal ageing nevertheless maintain sufficient support so as not to affect visual function during a normal lifespan.[28,29,32] In AMD, the decreased degradative capacity documented in the present study may lead to the advanced ageing changes capable of providing the initial metabolic insult that can progress to a pathologic change. Stimulation of the MMP pathway would therefore constitute a viable therapeutic option in the treatment and management of AMD patients.

We have demonstrated that in vitro addition of exogenously activated MMP2 and -9 can improve the functional aspects of Bruch's membrane.[54] Interestingly, active MMP2 was more effective in the younger subset than in the elderly, whereas active MMP9 showed a more rigorous impact that was much exaggerated in the elderly donor set.

Although little is known about the activation mechanism of pro-MMP9, clear differences exist compared to pro-MMP2. As indicated earlier, activation of pro-MMP2 requires the exogenous presence of TIMP2 and when TIMP2-containing medium (fetal calf serum) is removed, only pro-MMP2 is synthesized and is restricted to the interior of the RPE cell.[54] However, under the same serum-free conditions, pro-MMP9 is synthesized and converted to the active form. Thus the RPE cell is capable of converting pro-MMP9 to its activated form in response to physiological or pathologic signals. Physiologically, such signals may arise during migration of RPE cells either during cell culture or in response to a laser lesion when the surrounding RPE cells start migrating in an attempt to close the wound (Zhang J, et al. *IOVS* 2009;50:ARVO E-Abstract 3425).[54]

Specific targeting of RPE cells without collateral retinal damage with the newly introduced ultrashort-pulse laser system (Ellex R&D Pty, Ltd., Adelaide, SA, Australia) has shown the release of active MMP9 enzymes and early clinical trials appear to support the concept of reactivating the MMP system of Bruch's membrane in the treatment of AMD (Zhang J, et al. *IOVS* 2010;51:ARVO E-Abstract 525; Guymer RH, et al. IOVS 2010;51:ARVO E-Abstract 523).

References

1. Johansson N, Ahonen M, Kahari VM. Matrix metalloproteinases in tumour invasion. *Cell Mol Life Sci.* 2000;57:5–15.
2. Massova I, Kotra LP, Fridman R, Mobashery S. Matrix metalloproteinases: structures, evolution, and diversification. *FASEB J.* 1998;12:1075–1095.
3. Woessner JF. Matrix metalloproteinases and their inhibitors in connective tissue remodelling. *FASEB J.* 1991;5:2145–2154.
4. Matrisian LM. The matrix-degrading metalloproteinases. *Bioessays.* 1992;14:455–463.
5. Murphy G, Crabbe T. Gelatinases: A and B. *Methods in Enzymol.* 1995;248:470–484.
6. Birkedal-Hansen H, Moore WG, Bodden MK, et al. Matrix metalloproteinases: a review. *Crit Rev Oral Biol Med.* 1993;4:197–250.
7. Alexander JP, Bradley JMB, Gabourel JD, Acott TS. Expression of matrix metalloproteinases and inhibitor by human retinal pigment epithelium. *Invest Ophthalmol Vis Sci.* 1990;31:2520–2528.
8. Hunt RC, Fox A, Pakalnis VAL, et al. Cytokines cause cultured retinal pigment epithelium cells to secrete metalloproteinases and to contract collagen gels. *Invest Ophthalmol Vis Sci.* 1993;34:3179–3186.
9. Vranka JA, Johnson E, Zhu X, et al. Discreet expression and distribution pattern of TIMP-3 in the human retina and choroid. *Curr Eye Res.* 1997;16:102–110.
10. Guo L, Hussain AA, Limb GA, Marshall J. Age-dependent variation in metalloproteinase activity of isolated human Bruch's membrane and choroid. *Invest Ophthalmol Vis Sci.* 1999;40:2676–2682.
11. Fariss RN, Apte SS, Olsen BR, Iwata K, Milam AH. Tissue inhibitor of metalloproteinases-3 is a component of Bruch's membrane of the eye. *Am J Pathol.* 1997;150:323–328.
12. Weber BH, Vogt G, Pruett RC, Stohr H, Felbor U. Mutations in the tissue inhibitor of metalloproteinase-3 (TIMP-3) in patients with Sorsby's fundus dystrophy. *Nat Genet.* 1994;8:352–356.
13. Fariss RN, Apte SS, Luthert PJ, Bird AC, Milam AH. Accumulation of tissue inhibitor of metalloproteinases-3 in human eyes with Sorsby's fundus dystrophy or retinitis pigmentosa. *Br J Ophthalmol.* 1998;82:1329–1334.
14. Klenotic PA, Munier FL, Marmorstein LY, Apte BA. Tissue inhibitor of metalloproteinases-3 (TIMP-3) is a binding partner of epithelial growth factor-containing fibulin-like extracellular matrix protein1 (EFEMP1). *J Biol Chem.* 2004;279:30469–30473.
15. Marmorstein LY, Munier FL, Arsenijevic Y, et al. Aberrant accumulation of EFEMP1 underlines drusen formation in Malattia Leventinese and age-related macular degeneration. *Proc Natl Acad Sci USA.* 2002;99:13067–13072.
16. Ramratten RS, van der Schaft TL, Mooy CM, de Bruijn WC, Mulder PGH, de Jong PTVM. Morphometric analysis of Bruch's membrane, the choriocapillaris and the choroid in ageing. *Invest Ophthalmol Vis Sci.* 1994;35:2857–2864.
17. Okubo A, Rosa RH, Bunce CV, et al. The relationships of age changes in retinal pigment epithelium and Bruch's membrane. *Invest Ophthalmol Vis Sci.* 1999;40:443–449.
18. Karwatowski WSS, Jefferies TE, Duance VC, Albon J, Bailey AJ, Easty DL. Preparation of Bruch's membrane and analysis of the age related changes in the structural collagens. *Br J Ophthalmol.* 1995;79:944–952.
19. Handa JT, Verzijl N, Matsunaga H, et al. Increase in the advanced glycation end-product pentosidine in Bruch's membrane with age. *Invest Ophthalmol Vis Sci.* 1999;40:775–779.
20. Pauleikhoff D, Zuels S, Sheraidah G, Marshall J, Wessing A, Bird AC. Correlation between biochemical composition and fluorescein binding of deposits in Bruch's membrane. *Ophthalmology.* 1992;99:1548–1553.
21. Holz FG, Sheraidah GS, Pauleikhoff D, Bird AC. Analysis of lipid deposits extracted from human macular and peripheral Bruch's membrane. *Arch Ophthalmol.* 1994;112:402–406.
22. Kamei M, Hollyfield JG. TIMP-3 in Bruch's membrane: changes during aging and in age-related macular degeneration. *Invest Ophthalmol Vis Sci.* 1999;40:2367–2375.
23. Nagai N, Klimava A, Lee W-H, Izumi-Nagai K, Handa JT. CTGF is increased in basal deposits and regulates matrix production through the ERK (p42/p44 mapk) MAPK and the p38 MAPK signalling pathways. *Invest Ophthalmol Vis Sci.* 2009;50:1903–1910.
24. Yamada Y, Ishibashi K, Ishibashi K, et al. The expression of advanced glycation endproduct receptors in RPE cells associated with basal deposits in human maculas. *Exp Eye Res.* 2006;82:840–848.
25. Mott JD, Khalifah RG, Nagase H, Shield CF, Hudson JK, Hudson BG. Nonenzymatic glycation of type IV collagen and matrix metalloproteinase susceptibility. *Kidney Int.* 1997;52:1302–1312.
26. Hamlin CR, Kohn RR. Evidence for progressive, age-related structural changes in post-mature human collagen. *Biochim Biophys Acta.* 1971;236:458–467.
27. Vater CA, Harris ED, Siegel RE. Native cross-links in collagen fibrils induce resistance to human synovial collagenase. *Biochem J.* 1979;181:639–645.
28. Moore DJ, Hussain AA, Marshall J. Age-related variation in the hydraulic conductivity of Bruch's membrane. *Invest Ophthalmol Vis Sci.* 1995;36:1290–1297.
29. Starita C, Hussain AA, Pagliarini S, Marshall J. Hydrodynamics of ageing Bruch's membrane: Implications for macular disease. *Exp Eye Res.* 1996;62:565–572.
30. Hussain AA, Rowe L, Marshall J. Age-related alterations in the diffusional transport of amino acids across the human Bruch's-choroid complex. *J Opt Soc Am A.* 2002;19:166–172.
31. Moore DJ, Clover GM. The effect of age on the macromolecular permeability of human Bruch's membrane. *Invest Ophthalmol Vis Sci.* 2001;42:2970–2975.
32. Hussain AA, Starita C, Hodgetts A, Marshall J. Macromolecular diffusion characteristics of ageing human Bruch's membrane: Implications for age-related macular degeneration (AMD). *Exp Eye Res.* 201a;90:703–710.
33. Owsley C, Jackson GR, White M, Feist R, Edwards D. Delays in rod mediated dark adaptation in early age-related maculopathy. *Ophthalmology.* 2001;108:1196–1202.
34. Owsley C, McGwin G, Jackson GR, et al. Effect of short term, high-dose retinol on dark adaptation in age and age-related maculopathy. *Invest Ophthalmol Vis Sci.* 2006;47(4):1310–1318.
35. Steinmetz RL, Haimovici R, Jubb C, Fitzke FW, Bird A. Symptomatic abnormalities of dark adaptation in patients with age-related Bruch's membrane change. *Br J Ophthalmol.* 1993;77:549–554.
36. Chen JC, Fitzke FW, Pauleikhoff D, Bird A. Functional loss in age-related Bruch's membrane change with choroidal perfusion defect. *Invest Ophthalmol Vis Sci.* 1992;33:334–340.
37. Chau KY, Sivaprasad S, Patel N, Donaldson TA, Luthert PJ, Chong NV. Plasma levels of matrix metalloproteinase-2 and -9 (MMP2 and MMP9) in age-related macular degeneration. *Eye (Lond).* 2008;22:855–859.
38. Ye S. Polymorphism in matrix metalloproteinase gene promoters: implication in regulation of gene expression and susceptibility of various diseases. *Matrix Biol.* 2000;19:623–629.
39. Shimarjiri S, Arima N, Tanimoto A, et al. Shortened microsatellite d(CA)21 sequence down-regulates promoter activity of matrix metalloproteinase 9 gene. *FEBS Lett.* 1999;455:70–74.
40. Peters DG, Kassam A, St. Jean PL, et al. Functional polymorphism in the matrix metalloproteinase-9 promoter as a potential risk factor for intracranial aneurysm. *Stroke.* 1999;30:2612–2616.
41. Fornoni A, Wang Y, Lenz O, et al. Association of a decreased number of d(CA) repeats in the matrix metalloproteinase-9 promoter with glomerulosclerosis susceptibility in mice. *J Am. Soc Nephrol.* 2002;13:2068–2076.
42. Fiotti N, Pedio M, Battaglia PM, et al. MMP-9 microsatellite polymorphism and susceptibility to exudative form of age-related macular degeneration. *Genet Med.* 2007;4:272–277.
43. Kumar A, El-Osta A, Hussain AA, et al. Increased sequestration of matrix metalloproteinases in ageing human Bruch's membrane: implications for ECM turnover. *Invest Ophthalmol Vis Sci.* 2010;51:2664–2670.
44. Hussain AA, Lee Y, Marshall J. High molecular-weight gelatinase species of human Bruch's membrane: compositional analyses and age-related changes. *Invest Ophthalmol Vis Sci.* 2010;51:2363–2371.
45. Alcazar O, Cousins SW, Marin-Castano ME. MMP-14 and TIMP-2 over expression protects against hydroquinone-induced oxidant

injury in RPE: Implications for extracellular matrix turnover. *Invest Ophthalmol Vis Sci*. 2007;48:5662–5670.

46. Strongin AY, Collier I, Bannikov G, Marmer BL, Grant GA, Goldberg GI. Mechanism of cell surface activation of 72kDa type IV collagens: isolation of the activated form of the membrane metalloproteinase. *J Biol Chem*. 1995;270:5331–5338.
47. Smine A, Plantner JJ. Membrane type-1 matrix metalloproteinase in human ocular tissues. *Curr Eye Res.* 1997;16:925–929.
48. Butler GS, Butler MJ, Atkinson SJ, et al. The TIMP-2 membrane type I metalloproteinase 'receptor' regulates the concentration and efficient activation of progelatinase A: a kinetic study. *J Biol Chem*. 1998;273:871–880.
49. Marin-Castano ME, Csaky KG, Cousins SW. Nonlethal oxidant injury to human retinal pigment epithelial cells causes cell membrane blebbing but decreased MMP-2 activity. *Invest Ophthalmol Vis Sci.* 2005;46:3331–3340.
50. Leu ST, Batni S, Radeke MJ, Johnson LV, Anderson DH, Clegg DO. Drusen are cold spots for proteolysis: expression of matrix metalloproteinases and their tissue inhibitor proteins in age-related macular degeneration. *Exp Eye Res.* 2002;74:141–154.
51. Fini ME, Girard MT, Matsubara M, Bartlett JD. Unique regulation of the matrix metalloproteinase, gelatinase B. *Invest Ophthalmol Vis Sci.* 1995;36:622–633.
52. St. Jean PL, Zhang XC, Hart BK, et al. Characterisation of a dinucleotide repeat in the 92 kDa type IV collagenase gene (CLG4B), localisation of CLG4B to chromosome 20 and the role of CLG4B in aortic aneurysmal disease. *Ann Hum Genet.* 1995; 59:17–24.
53. Yoon S, Tromp G, Vongpunsawad S, Ronkainen A, Juvonen T, Kuivaniemi H. Genetic analysis of MMP3, MMP9, and PAI-1 in Finnish patients with abdominal aortic or intracranial aneurysms. *Biochem Biophys Res Commun.* 1999;265:563–568.
54. Ahir A, Guo L, Hussain AA, Marshall J. Expression of metalloproteinases from human retinal pigment epithelium cells and their effects on the hydraulic conductivity of Bruch's membrane. *Invest Ophthalmol Vis Sci*. 2002;43:458–465.